

Equilibrium and Computational Chemical Modelling Studies for the Removal of Methyl Orange and Methyl Red Dyes from Water Using Modified Silica Resin

Ranjhan Junejo, Nida Shams Jalbani, Savas Kaya, Sultan Erkan, Riadh Marzouki & Shahabuddin Memon

To cite this article: Ranjhan Junejo, Nida Shams Jalbani, Savas Kaya, Sultan Erkan, Riadh Marzouki & Shahabuddin Memon (2023) Equilibrium and Computational Chemical Modelling Studies for the Removal of Methyl Orange and Methyl Red Dyes from Water Using Modified Silica Resin, International Journal of Environmental Analytical Chemistry, 103:19, 8000-8016, DOI: [10.1080/03067319.2021.1979534](https://doi.org/10.1080/03067319.2021.1979534)

To link to this article: <https://doi.org/10.1080/03067319.2021.1979534>



Published online: 23 Sep 2021.



Submit your article to this journal [↗](#)



Article views: 220



View related articles [↗](#)




View Crossmark data [↗](#)



Citing articles: 7 View citing articles [↗](#)



Equilibrium and Computational Chemical Modelling Studies for the Removal of Methyl Orange and Methyl Red Dyes from Water Using Modified Silica Resin

Ranjhan Junejo ^a, Nida Shams Jalbani ^a, Savas Kaya^b, Sultan Erkan ^c,
Riadh Marzouki^d and Shahabuddin Memon^a

^aNational Centre of Excellence in Analytical Chemistry, University of Sindh, Jamshoro, Pakistan; ^bDepartment of Pharmacy, Health Services Vocational School, Sivas Cumhuriyet University, Turkey; ^cDepartment of Chemistry, Faculty of Science, Sivas Cumhuriyet University, Turkey; ^dDepartment of Chemistry, College of Science, King Khalid University, Abha, Saudi Arabia

ABSTRACT

This study describes the removal of methyl orange (MO) and methyl red (MR) dyes from water samples using morpholinomethylcalix[4]arene immobilised silica (MIS) resin. The silica surface has been modified by *p*-morpholinomethylcalix[4]arene moiety and was characterised by FT-IR spectroscopy and SEM techniques. The adsorption capacity of MIS-resin was checked through batch adsorption experiments under the optimised conditions of pH, MIS-resin dose, time, and temperature. Results show that adsorption of MO and MR dyes are highly affected by the change in pH; thus, the higher adsorption percentages were achieved at pH 5.3 and 6.6 respectively. The adsorbent dosage has been optimised and it was noticed that the maximum adsorption was achieved by using 40 mg.L⁻¹ of MIS-resin dose. The adsorption rate of dyes was investigated by applying the pseudo-first and second-order kinetic models and it has been observed that the experimental data shows a better correlation coefficient with the pseudo-second-order kinetic model. The feasibility of adsorption was analysed by thermodynamic parameters such as ΔH° , ΔG° , and ΔS° values indicate that the adsorption of dyes is exothermic and spontaneous. The equilibrium data have been validated using Langmuir and Freundlich models and the Langmuir model has a good correlation coefficient (R^2 0.99). The MIS-resin was applied onto industrial effluents and it has been observed that the prepared resin is a very efficient adsorbent for the treatment of dyes contaminated wastewater. The adsorption of MO and MR dyes onto MIS-resin was well defined by computational chemical modelling at the B3LYP/LANL2DZ/6-311++G(d,p) level using G09W software.

ARTICLE HISTORY

Received 22 May 2021
Accepted 2 September 2021

KEYWORDS

DFT and computational chemical calculations; calix [4]arene; silica resin; methyl orange and methyl red dyes; equilibrium; kinetic and thermodynamic modelling studies

1. Introduction

Dyes are widely used in textile, paper, pharmaceutical, food, cosmetics, and chemical industries respectively [1]. Synthetic colourants are highly stable towards the light, biodegradation, and oxidation reaction due to their complex chemical structure and synthetic origin, which enhance their application in the industrial sector. It has been

estimated that the per-year production of dyes is above 7×10^5 , of which 10–15% are discharged as effluents in freshwater [2]. Discharge of a huge amount of synthetic dyes in freshwater produces undesirable serious environmental impact. Though the release of these colours at very low concentrations causes serious disaster to aquatic and human beings. Synthetic dyes in freshwater stop sunlight and oxygen penetration due to their deep colour and causes derogatory effects on the photosynthetic-activity of an aquatic system [3]. Therefore, it is necessary to treat the industrial effluents before drained into freshwater. In this regard, many techniques were developed for the treatment of dyes contaminated water such as adsorption, membrane, reverse osmosis, oxidation, electrochemical, coagulation and fluctuation. However, adsorption has proved to be a cheaper, simple, easier, and most efficient process for the decontamination of wastewater [4–7].

For the effective removal of dyes from wastewater, the adsorbent should be inexpensive, stable, regenerable, and efficient [8–11]. Previously different adsorbents have been used for the adsorptive removal of dyes. Adsorbents can be classified as organic (natural polymers/synthetic polymers) and inorganic (silica SiO_2 , alumina Al_2O_3 , MgO , etc.). Inorganic adsorbents based on SiO_2 have commonly used adsorbents for water pollutants due to their thermal and chemical stability towards different environmental conditions. The surface of silica is comprised of silanol groups which can be modified by immobilisation of organic moieties [12]. The modified silica has better adsorption efficiency, selectivity, stability, and high adsorption capacity, which is applicable for the treatment of a wide variety of water pollutants. The silica surface can be modified by different organic compounds but the attachment of calix[n]arene derivatives increases their application in the field of separation science and technology [13–16].

The calixarenes are cyclic oligomers prepared from the base-catalysed reaction of phenol and formaldehyde. The calixarenes are comprised of upper and lower rims that can be functionalised by a variety of functional groups [17–19]. In literature, calixarenes modified silica-based adsorbents have been used for the adsorption/removal of dyes such as p-tert-butylcalix[4]arene and p-tert-butylcalix[8]arene immobilised on silica surface for the adsorption of RB-5 and RR-45 dyes from water [20,21]. Another study was performed using calix[4]arene-based resin for the removal of methyl orange and methyl red dyes from water under the optimised parameters [22]. In another study, the lead sulphide modified calix[6]arene was used as an efficient regenerable adsorbent for the methylene blue dye [23], while the cationic dyes (methylene blue and toluidine blue) were removed using calix[4]arene cross-linked polymer [24]. In our previous studies many calix[4]arene based resin have been reported for the removal of dyes such as piperdinomethylcalix[4]arene silica resin was applied for the removal of RB-19 dye [25], p-diethanolaminomethylcalix[4]arene immobilised silica (DIS) resin used for removal of the DB-38 dye [26], and calix[4]arene-silica resin was utilised for the adsorption of RY-18, RR-2, RB-13, and RB-171 dyes [27].

Herein, we have evaluated the application of morpolinomethylcalix[4]arene immobilised silica resin for the removal of methyl orange and methyl red dyes from water. In addition, the density functional theory (DFT) based calculations were also performed to describes the adsorbent and adsorbate interaction.

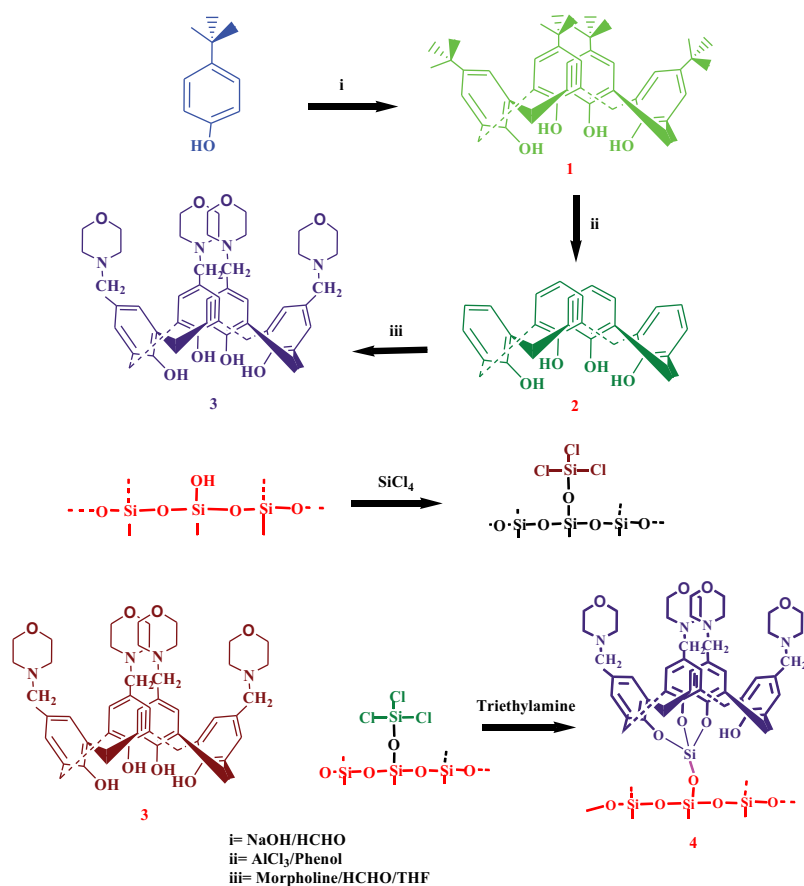
2. Materials and Methods

2.1. Chemicals and Instrumentations

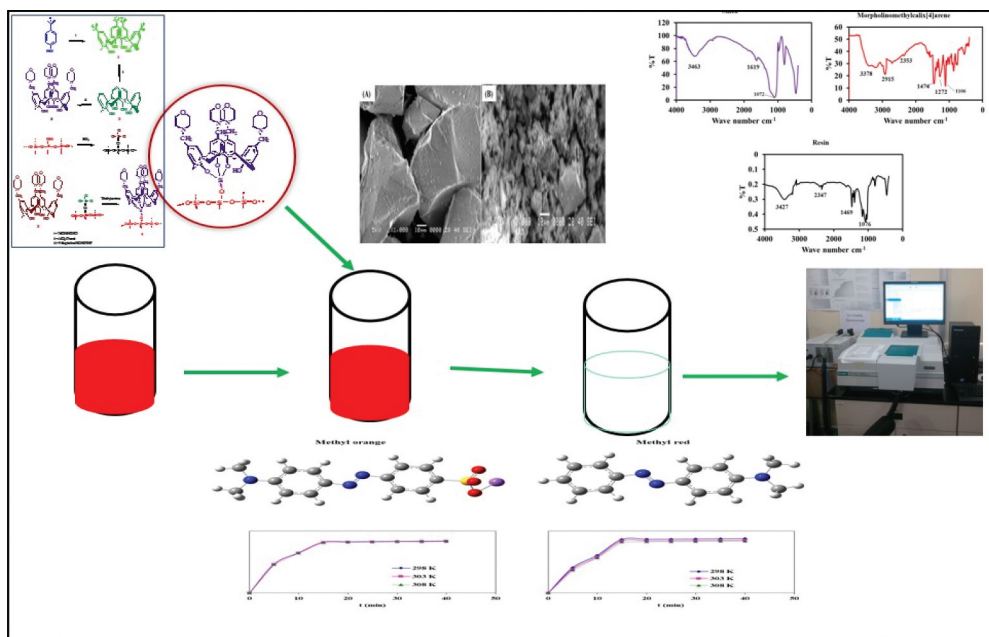
The methyl orange and methyl red dyes were purchased by Merck Company. The real dye contaminated water samples have been obtained from local textile industries of Karachi-Sindh Pakistan. The 0.1 M HCl/NaOH solutions were used to adjust the pH of the dye solution. Thermo Nicolet 5700 FTIR spectrometer (WI. 53,711, USA) have been used for FTIR purpose. JSM-6380 instrument used to perform Scanning electron microscopic (SEM) studies. UV-VIS spectrophotometer (Agilent Carry-100) was used for UV/VIS analysis. The pH metre (wtw) is used for pH measurement.

2.2. Synthesis

The compounds (**1–4**) shown in [scheme 1](#) have been prepared according to previously reported methods [13,28,29].



Scheme 1. Synthesis route of morpholinomethylcalix[4]arene immobilised silica resin.



Scheme 2. The schematic representation of synthesis of MIS-resin and equilibrium experiments.

2.3. Adsorption Methodology

Batch adsorption methodology was applied to check the adsorption efficiency of MIS resin. During equilibrium experiments, the pH, concentration, dosage, and effect of temperature were optimised. Thus, different doses were examined ranging from 10–50 mg/10 mL of dyes keeping other parameters constant. The pH of the dye solutions were optimised from acidic to basic using NaOH and HCl (0.1 M). The dye solutions were equilibrated on the mechanical shaker at 25°C, rpm 130 for 60 minutes by adding an optimised resin dose. The MIS resin from the solutions was filtered and remaining concentrations were analysed by ultraviolet-visible spectrophotometer and % adsorption and (q_e) were calculated using equations 1 and 2 (Scheme 2).

$$\% \text{ Adsorption} = \frac{C_i - C_f}{C_i} \times 100 \quad (1)$$

$$q_e = \frac{(C_i - C_e)V}{m} \quad (2)$$

Where C_i and C_f is the initial and final concentration (ppm), V is the volume (mL) of dyes and m is the mass of MIS-resin in (mg).

2.4. Computational study

The highest occupied molecular orbital energy (EHOMO), lowest empty molecular orbital (ELUMO), energy gap (E), hardness (η), softness (σ), electronegativity (χ), chemical potential (μ), electrophilic index (ω), nucleophilicity (ϵ), electron acceptance power (ω^+),

electron donation power (ω^-), electron transfer fractions (ΔN) and polarisability (α) of the studied dyes were investigated by Conceptual Density Functional Theory (CDFT). The ionisation energy (I) and electron affinity (A) specified in theory are presented through the following equations 3 and 4 [30].

$$I = -E_{HOMO} \quad (3)$$

$$A = -E_{LUMO} \quad (4)$$

The hardness (η), softness (σ), electronegativity (χ), chemical potential (μ) were calculated from the following equations 5–7 [31].

$$\eta = \frac{1}{2} \left[\frac{\partial^2 E}{\partial N^2} \right]_{v(r)} = \frac{I - A}{2} \quad (5)$$

$$\sigma = 1/\eta \quad (6)$$

$$\mu = -\chi = \left[\frac{\partial E}{\partial N} \right]_{v(r)} = -\left(\frac{I + A}{2} \right) \quad (7)$$

An electrophilic index (ω) based on chemical hardness and electronegativity was calculated by equation 8 [32]. The nucleophilicity (ε) is a form of electrophilicity index equation 9.

$$\omega = \chi^2/2\eta \quad (8)$$

$$\varepsilon = 1/\omega \quad (9)$$

Electron accepting (ω^+) and electron donating (ω^-) power values, depending on the ionisation energy and electron affinity of the inhibitory molecules can be calculated using equation 10 and 11 [33].

$$\omega^+ = (I + 3A)^2/(16(I - A)) \quad (10)$$

$$\omega^- = (3I + A)^2/(16(I - A)) \quad (11)$$

The polarisability (α) is calculated using equation 12 based on the diagonal components of the polarisability tensor.

$$\langle \alpha \rangle = 1/3 [\alpha_{xx} + \alpha_{yy} + \alpha_{zz}] \quad (12)$$

3. Results and Discussion

3.1. Characterisation

3.1.1. FT-IR Spectroscopy

FTIR spectroscopy is an analytical technique commonly used for functional group analysis. In this study, FTIR analysis has been performed (Figure 1) in which spectrum of silica has peaks at 3464, 1619 cm^{-1} for Si-OH and Si-O stretching respectively; while the peaks at 1072 cm^{-1} is of OH bending. The spectrum of morpholinomethylcalix[4]arene has been

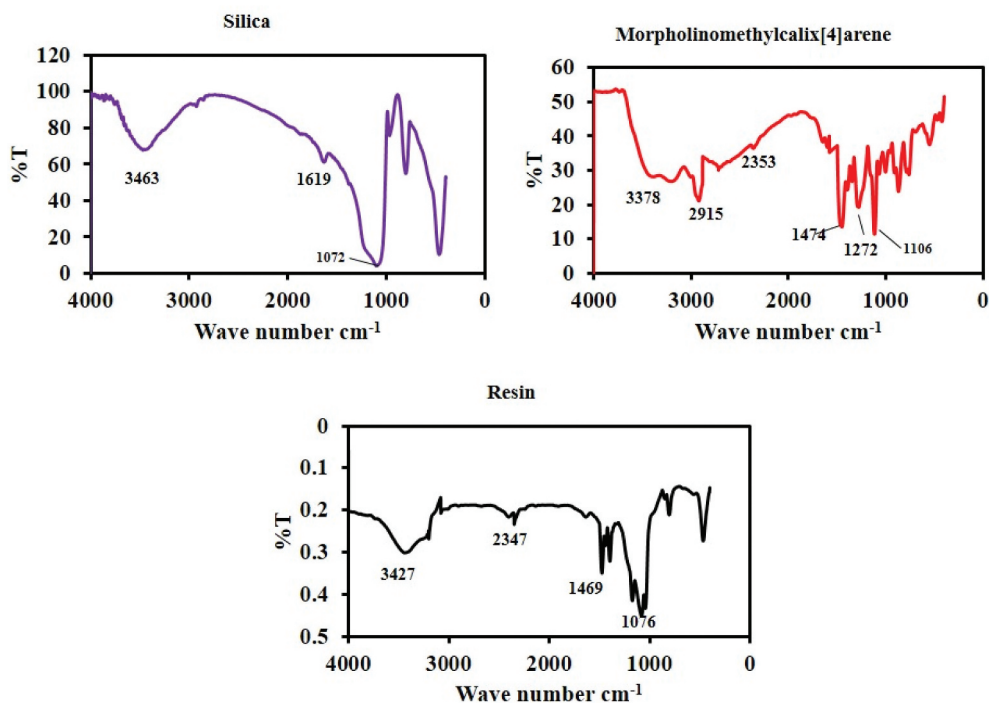


Figure 1. FTIR spectra of silica, morpholinomethylcalix[4]arene and MIS-resin.

characterised by the peaks at 3378, 2915, 2353, 1474 and 1272 for OH, C-H, C = C, C-O and C-N stretching frequencies respectively; while 1102 is OH bending frequency. The spectrum of MIS-resin has new peaks at 3427, 2347, and 1469 cm^{-1} for OH, C = C, C-O stretching frequencies respectively while the peak at 1076 is of OH bending frequency.

3.1.2. Scanning Electron Microscopy (SEM) Characterisation

Figure 2 shows the SEM images of pure silica and MIS-resin. Image (A) is of silica surface which is smooth and crystalline while image (B) is of MIS-resin which is rough amorphous. The roughness of the MIS-resin surface is formed due to the immobilisation of morpholinomethylcalix[4]arene onto the silica surface.

3.2. Resin Dosage

The resin doses were optimised from 10–50 mg.L^{-1} at the constant concentration (5ppm) as shown in Figure 3. It is clear that the adsorption percentage increases by increasing the MIS-resin dosage and then becomes constant after 40 mg.L^{-1} . The addition of a further higher amount of resin does not affect % adsorption, thus all the experiments were performed at 40 mg.L^{-1} . In previous studies, the calix[4]arene-based silica resins were used for the adsorption of dyes such as adsorption of congo red was performed using 100 mg.L^{-1} of calix[4]arene-based resin [34]. Similarly, the adsorption of RB-19 dye was

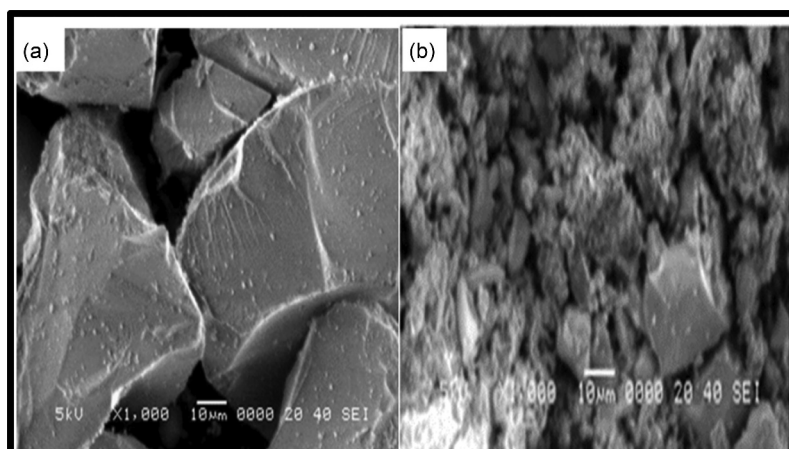


Figure 2. SEM images of pure silica (A) and MIS-resin (B).

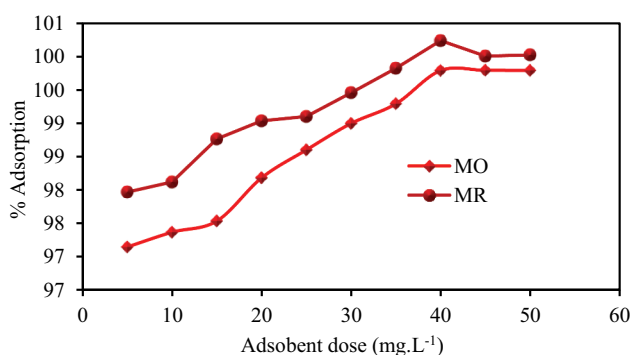


Figure 3. Effect of resin dosage on adsorption percentage of MO and MR dyes.

performed using 25 mg.L⁻¹ of calix[4]arene-based resin [25]. Moreover, the p-sulphona-tocalix[8]arene silica-resin was applied for the adsorption of MB dye from water using 50 mg.L⁻¹ of resin for maximum % adsorption [35].

3.3. Effect of pH

The pH of the solution is important in adsorption because it has a major role in the attraction of adsorbate species on the adsorbent material. Herein, the pH of MO and MR dyes have been optimised from acidic to basic range as shown in Figure 4. It has been observed in Figure 4, that the adsorption percentage of MO and MR dyes are maximum at acidic to neutral pH and decreases in basic media. Thus, it can be said that at basic pH, negatively charged binding sites enhanced at dye molecule as well as resin surface that may produce electrostatic repulsion forces and due this repulsion adsorption percentage decreases at higher pH value. At low pH, H⁺ ions are present in excess on dye molecule sites that produce an electrostatic attraction towards electron-donating moieties such as nitrogen and oxygen group present onto resin surface. By increasing the pH of solution,

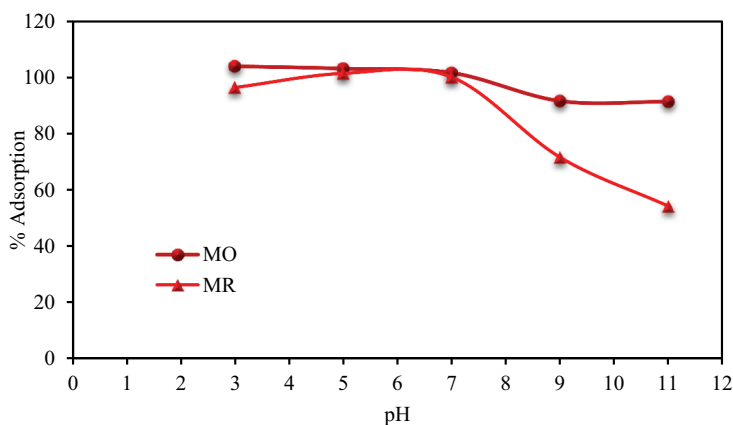


Figure 4. Effect of pH on the adsorption percentage of MO and MR dyes.

the number of positive ions is decreased and less attraction has been observed. In previous studies, the adsorption dyes have been performed using calix[4]arene based adsorbent and it has been observed that the maximum adsorption was obtained at the acidic to neutral pH. The adsorption of (DB15) and Chicago sky blue (CSB) has been performed at pH 2.0–5.2 using calix[4]arene-based copolymer adsorbent [36]. The adsorption of RB-19 dye using calix[4]arene based silica resin was performed at the acidic to neutral pH [25]. In addition, the calix[4]arene XAD-4-resin was used for the adsorption of methyl orange and methyl red dyes from water at acidic to neutral pH [22].

3.4. Adsorption kinetics study

The kinetic study of MO and MR dyes has been evaluated on MIS-resin. The kinetic experiments were conducted by adding 40 mg of MIS-resin into a flask containing 10 mL of each dye solution. The uptake process of dyes using MIS-resin was examined at different time intervals (5 – 120 min) at 298–308 K and after completion, the MIS-resin was filtered off through filter paper. The kinetic data and rate of reaction were calculated using pseudo-first-order and pseudo-second-order models respectively. The linear forms of these models are given as equations 14 and 15.

$$\ln(q_e - q_t) = \ln q_e - k_1 t \quad (14)$$

$$\frac{t}{q_t} = \left(\frac{t}{k_2 q_e^2} \right) + \left(\frac{1}{q_e} \right) \quad (15)$$

Where q_t and q_e (mol/g) are the adsorbed amount of dyes at time t (min) and at an equilibrium respectively while the k_2 (g/mol.min⁻¹) and k_1 (1/min) are rate constants of both models, respectively. The effect of contact time on adsorption percentage at various temperatures is shown in Figure 5 for methyl orange and methyl red dyes. It has been observed that the adsorption percentage increases initially and then becomes constant

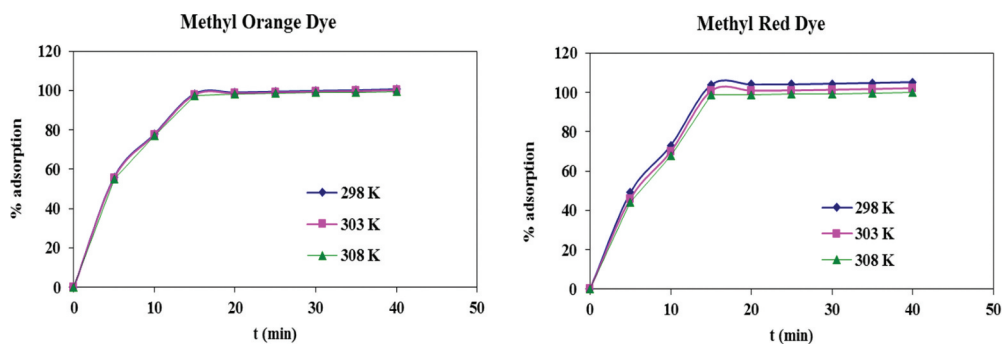


Figure 5. Effect of contact time on the adsorption of methyl orange (MO) and methyl red (MR) dyes by resin at various temperature.

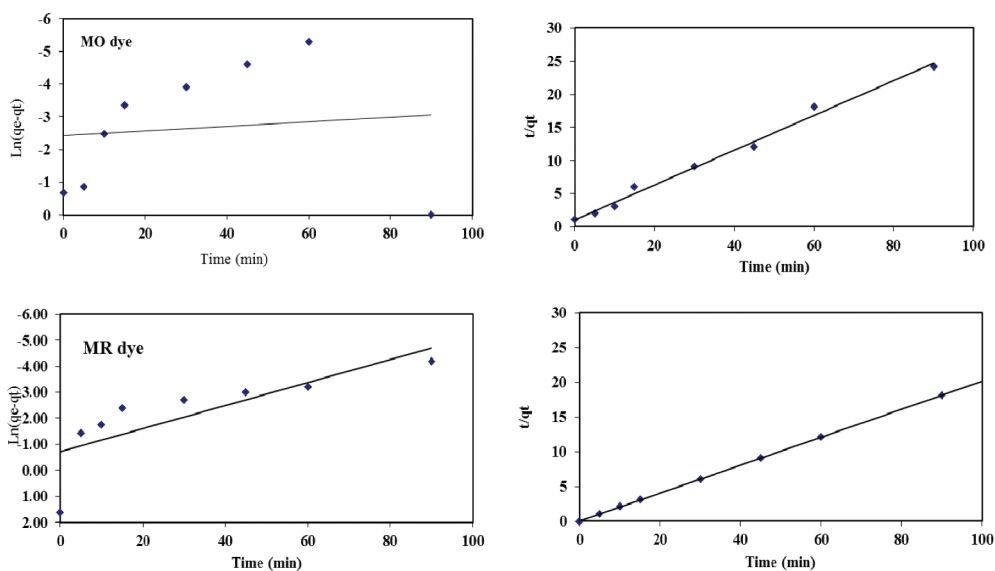


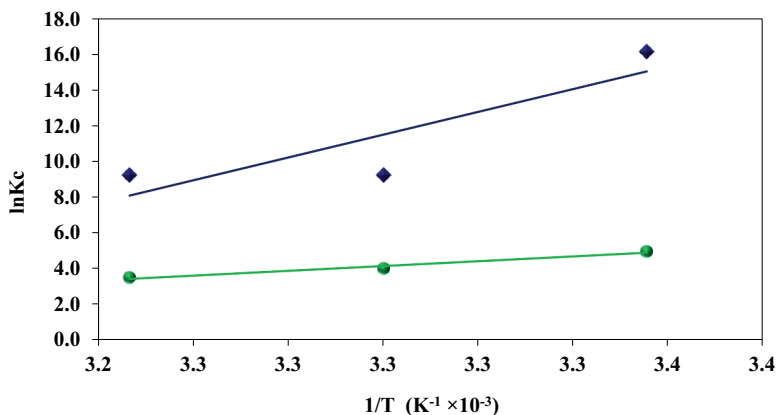
Figure 6. The plot of pseudo first and second order kinetic model for the adsorption of methyl orange (MO) and methyl red (MR) dyes by MIS-resin at 298 K.

after 15 minutes because after 15 minutes almost dyes concentrations have been adsorbed. Moreover, the adsorption percentage was also slightly decreased with temperature increasing the temperature (298 to 308 K).

The rate of adsorption was fast initially and then becomes constant after 15 min due to availability of a large number of binding sites of the resin surface. The linear fitting of pseudo first and second kinetic models are shown in Figure 6 at 298 K clearly describes the fitting of the pseudo second order model very well. The corresponding parameters of both models are given in Table 1. In Table 1 the methyl orange and methyl red dyes show very poor correlation coefficient values while both dyes have better correlation coefficient values ($R^2=0.999$). Thus results suggest that the adsorption of methyl orange and methyl red dyes follows the pseudo second order kinetic model very well.

Table 1. The kinetic parameters of pseudo-first-order and pseudo-second-order for the MO and MR dyes adsorption onto resin.

Dyes	Pseudo first order			Pseudo second order		
	q_e (mg.g ⁻¹)	K_f (min ⁻¹)	R^2	q_e (mg.g ⁻¹)	K_2 (g.mg ⁻¹ .min ⁻¹)	R^2
MO dye	0.42	0.0019	0.843	3.80	0.119	0.991
MR dye	0.73	0.0013	0.566	4.99	1.634	0.999

**Figure 7.** Van't Hoff plot for the adsorption of MO and MR dyes on MIS-resin.**Table 2.** Thermodynamic parameters for the adsorption of MO and MR dyes onto MIS-resin.

Dyes	ΔH (KJ/mol)	ΔS (KJ/mol)	ΔG (KJ/mol)		
			298 K	303 K	308 K
MR	-0.524	-1.646	-39.91 $\ln K_c = 16.1$	-23.57 $\ln K_c = 9.2$	-23.19 $\ln K_c = 9.2$
MO	-0.112	-0.334	-12.23 $\ln K_c = 4.9$	-10.04 $\ln K_c = 4.0$	-8.90 $\ln K_c = 3.5$

3.5. Thermodynamic study

The thermodynamic parameters (ΔH , ΔG and ΔS) are the most important parameters for the adsorption of methyl orange and methyl red dyes from water by MIS-resin. The values of ΔH , ΔG and ΔS determine the spontaneous or non-spontaneous nature of the reaction. The thermodynamic parameters can be calculated from the following equations 16 and 17.

$$\ln k_c = \frac{-\Delta H}{RT} + \frac{\Delta S}{R} \quad (16)$$

$$\Delta G = -RT \ln k_c \quad (17)$$

Where $\ln k_c$ is the thermodynamic equilibrium constant, T is the temperature in Kelvin and R is the ideal gas constant (8.314 J.mol⁻¹.K⁻¹). The values of ΔG and ΔS were calculate obtained from the slope and intercept of the graph $\ln k_c$ vs $1/T$ as shown in Figure 7.

The constant values of thermodynamic parameters are given in Table 2. The negative values of ΔG demonstrate that the adsorption of MO and MR dye is spontaneous and decreasing the negative values with increasing the temperature suggests that adsorption

is not favourable at the higher temperature. The values of ΔH for MR (-0.524) and MO (-0.112) indicate that the adsorption of dyes onto resin is exothermic while the values of $(-\Delta S)$ for both dyes indicate that the randomness increased at the solid surface in solution [37].

3.6. Adsorption isotherm

To describe the adsorption capacity as well as physical or chemical nature of adsorption; two models (Langmuir and Freundlich) are generally applied to experimental data. The linear form of both models is given in equations 18 and 19.

$$\left(\frac{C_e}{C_{ads}}\right) = \left(\frac{1}{Qb}\right) + \left(\frac{C_e}{Q}\right) \quad (18)$$

$$\log C_{ads} = \log A + \left(\frac{1}{n}\right) \log C_e \quad (19)$$

Where C_e is the equilibrium concentration, C_{ads} is adsorbed concentration. The Q (mg.g^{-1}) is the adsorption capacity of resin. In equation 19 A is the adsorption capacity and $1/n$ is adsorption intensity.

The isotherm models of MO and MR are shown in Figure 8 and it has been noticed that the adsorption capacity is increasing with increasing initial concentrations of both dyes and becomes constant after saturation of MIS-resin surface. All the constant parameters of both models are given in Table 3. From the table, it is clear that the linear correlation coefficients calculated from the Freundlich equation were less as compared to the Langmuir model. It can be observed obviously that the Langmuir isotherm model for MO and MR dyes could better describe the equilibrium data.

3.7. Computational details

3.7.1. Optimised structure

Methyl orange and methyl red compounds are optimised at B3LYP/6-31 G(d) levels. Optimised structures of compounds studied were given in Figure 9.

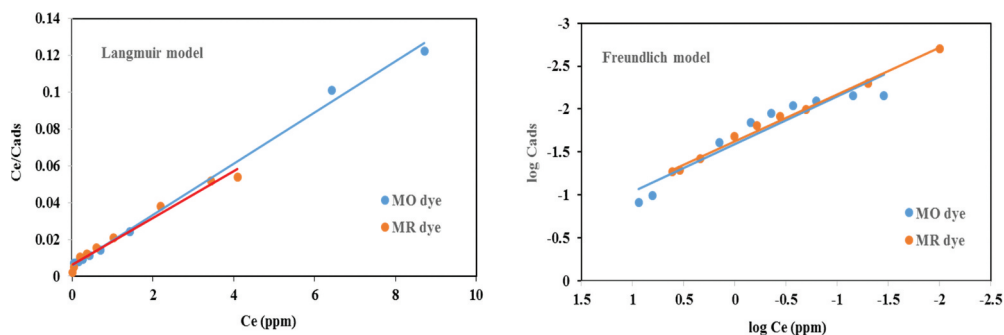
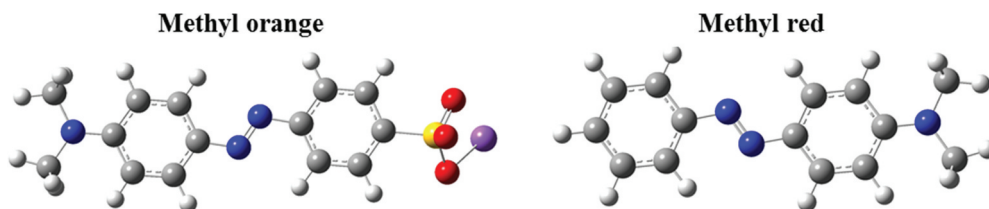


Figure 8. Langmuir and Freundlich isotherm models for the adsorption of MO and MR dyes from water.

Table 3. Langmuir, Freundlich, adsorption isotherm parameters.

Parameters	Langmuir Model	Freundlich Model
MO dye		
Q (mg.g^{-1})	175.4	-
b (L.mg^{-1})	0.41	-
A	-	0.026
$1/n$	-	0.556
R^2	0.996	0.890
MR dye		
Q (mg.g^{-1})	156.25	-
b (L.mg^{-1})	0.51	-
A	-	9.290
$1/n$	-	0.572
R^2	0.978	0.919

**Figure 9.** Optimised structures of compounds studied.**Table 4.** The calculated quantum chemical descriptors at B3LYP/6-31 G(d) level .

	Methyl orange	Methyl red
E_{HOMO} (eV)	-5.1169	-5.0809
E_{LUMO} (eV)	-1.8264	-1.7200
ΔE (eV)	3.2904	3.3609
η (eV)	1.6452	1.6805
σ (eV^{-1})	0.6078	0.5951
χ (eV)	3.4717	3.4005
μ (eV^{-1})	-3.4717	-3.4005
ω	3.6629	3.4406
ε	0.2730	0.2907
ω^+	1.3714	1.2901
ω^-	5.6040	5.3510
ΔN	0.4098	0.4224
α	270.09	218.62

3.7.2. Chemical reactivity analysis

For the studied dye molecules, calculated (E_{HOMO}), (E_{LUMO}), energy gap (ΔE), hardness (η), softness (σ), electronegativity (χ), chemical potential (μ), electro accepting power (ω^+), electro donating power (ω^-) and polarisability (α) values obtained using the B3LYP method and 6-31 G(d) basis set of Density Function Theory (DFT) are listed in Table 4.

The chemical hardness can be explained as 'the resistance against electron cloud polarization of compounds' [38]. This quantity is one of the important descriptors considered in the reactivity analysis of chemical species. The hard molecules have low electron donating capability. According to maximum hardness principle [39]

imparted to science after hard and soft acid-base principle (HSAB) by Pearson, a chemical system at equilibrium wants to reach to the state of maximum hardness. It can be understood from here that chemical hardness is a measurement of the molecular stability. Soft molecules have high electron donating capability. In the light of the data presented in table 4, one can say that methyl red dye is more stable with respect to methyl orange dye. Ghosh and co-workers proposed that softness is proportional to the cube root of the polarisability. According to minimum polarisability principle introduced within the framework of maximum hardness principle, in a stable state, polarisability is minimised [40]. Polarisability values also support the agreement between Maximum Hardness and Minimum Polarisability Principle because the polarisability values of methyl orange and methyl red dyes are 218.62 and 270.9 au, respectively.

Last electronic structure principle providing information about the reactivity of molecules is minimum electrophilicity principle states that in a chemical reaction, the sum of the electrophilicity indexes of products should be smaller than the sum of the electrophilicity indexes of reactants. From here, it can be concluded that in a stable state, electrophilicity also is minimised like polarisability. This principle also implies that methyl red dye is more stable compared to methyl orange dye.

3.7.3. Frontier molecular orbitals and molecular electrostatic potential

The HOMO, LUMO and the HOMO-LUMO energy gap are parameters representing chemical reactivity. The green and dark red isolates of HOMO and LUMO show the electron density in the molecule with positive and negative values, respectively. The molecular orbital energy diagram for HOMO and LUMO is shown in Figure 10. According to the contour diagrams of the orbitals, although the HOMO molecular orbital is concentrated on all molecules, the size of the lobes in the phenyl ring is remarkable. When LUMO molecular orbitals are examined, it is seen that they have the properties of π^* molecular orbitals

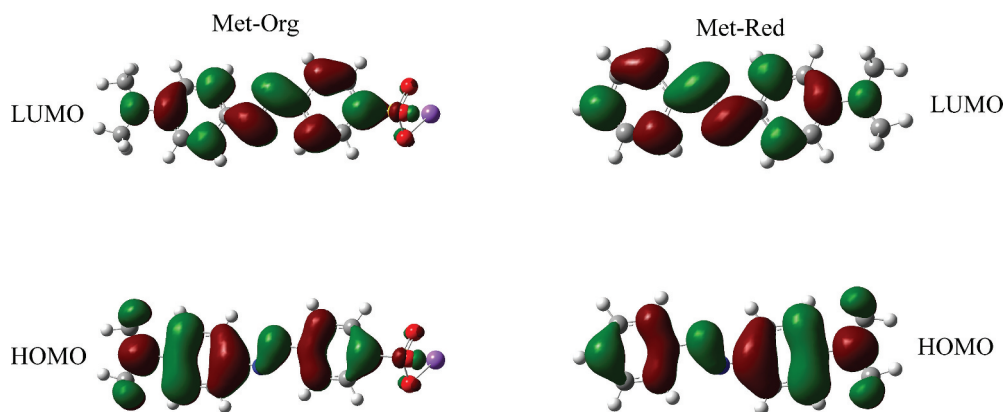


Figure 10. Frontier molecular orbitals of investigated molecules.

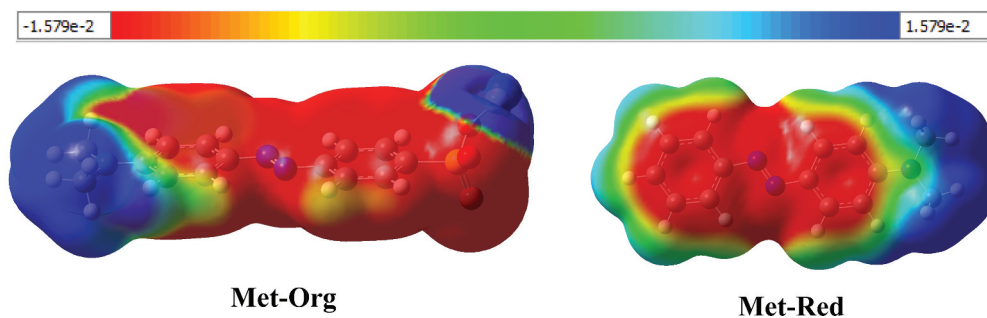


Figure 11. MEP maps of MO and MR dye molecule.

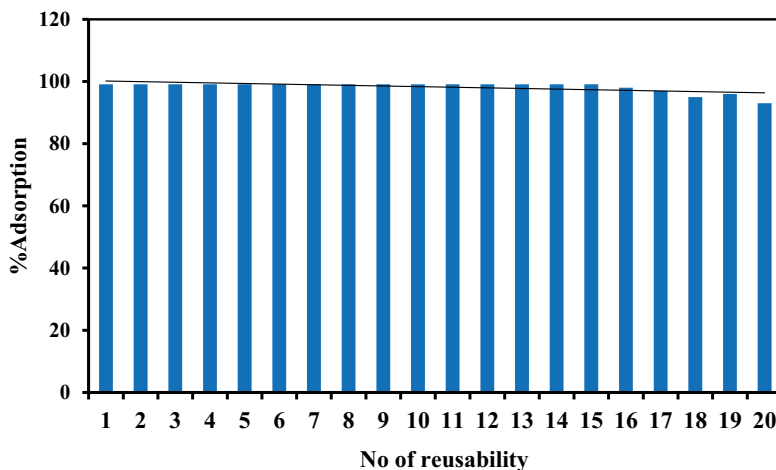


Figure 12. The number of reusability cycles of MIS-resin.

It provides information on molecular electrostatic potential (MEP), molecular electron density and qualitative interpretation of chemical reactivity. MEPs are used to predict and interpret both electrophilic and nucleophilic regions. MEP maps of the compounds studied are shown in [Figure 11](#).

The red coloured regions represent negatively charged areas of the molecule surface. It can accept an electrophile to red areas. The red regions in the compounds are concentrated on the oxygen atom. In addition, nucleophilic reactivity regions in the maps are indicated by the positive (light blue) regions of the MEP.

3.8. Reusability of MIS-resin

The most important feature of MIS-resin is reusability by washing with the mixture of methanol and water by 1:4 respectively. [Figure 12](#) demonstrates that there is no significant change noticed in the adsorption percentage of MIS-resin after many of cycles of its reusability.

Table 5. The % removal of MO and MR dyes from wastewater samples.

MO dye Sample	Concentration (ppm) before adsorption	Concentration (ppm) after adsorption	% Removal
1	0.200	0.016	92.000
2	0.188	0.013	93.085
3	0.430	0.052	87.907
MR dye Sample	Concentration (ppm) before adsorption	Concentration (ppm) after adsorption	% Removal
1	0.0330	0.0010	96.969
2	0.0661	0.0021	96.823
3	0.0081	0.0002	97.531

3.9. Real Water Sample Analysis

The capacity of MIS-resin was checked by analysing the water sample obtained from textile industrial effluents of Karachi-Sindh, Pakistan. Results show that the 40 mg/50 mL of MIS-resin is enough to adsorb above 90% of dyes from water sample [Table 5](#).

Adsorbent	Dyes	q_e ($mg.g^{-1}$) or % adsorption	Time (min)	pH	Reference
Pillar[5]arene-modified zeolite (PANI)-coated graphene oxide doped with SrTiO ₃ nanocube nanocomposites	Methyl orange	8.33 $mg.g^{-1}$ (85%)	150	5 and 9	[41]
	Methylene blue and Methyl orange (MO)	99% and 91 respectively	30	7	[42]
p-Sulphonatocalix[8]arene functionalised silica resin	Methylene blue	94%	10	9.5	[35]
Organo-modified silkworm exuviae	Methyl orange	87.03 $mg.g^{-1}$	60	3	[43]
MIS-resin	Methyl orange and Methyl red	175.4 and 154.6 $mg.g^{-1}$ respectively	15	5.3 and 6.6 respectively	Current study

3.10. Comparative Study

The results obtained during the experiments were compared with other published literature given in [Table 6](#). It is clear in [table 6](#) that MIS resin has comparable capacities for MO and MR dyes under the optimized parameters.

4. Conclusion

This study demonstrates the application of MIS-resin for the adsorption of methyl orange and methyl red dyes from water. The resin has good efficiency and high adsorption percentages for both dyes under the optimised parameters. Moreover, the experimental data follows a pseudo second order kinetic model with a good correlation coefficient value ($R^2=0.99$). The thermodynamic parameters determine that the adsorption of MO and MR dyes onto resin is exothermic and spontaneous. Equilibrium adsorption models show that the Freundlich model was the best fit as compared to the Langmuir model. The adsorption phenomenon of dyes and resin was highlighted by the DFT calculations. The resin was also applied on real waste water samples and it is clear that the resin has good efficiency to treat dyes contaminated wastewater.

Acknowledgments

Authors are thankful to National Centre of Excellence in Analytical Chemistry, University of Sindh Jamshoro, Pakistan, for facilitating this work. Authors are also extend their appreciation to the Deanship of Scientific Research at King Khalid University for funding this work through research group under grant number R.G.P1/173/42.

Disclosure statement

No potential conflict of interest was reported by the author(s).

ORCID

Ranjhan Junejo  <http://orcid.org/0000-0002-0090-1146>

Nida Shams Jalbani  <http://orcid.org/0000-0002-2435-0692>

Sultan Erkan  <http://orcid.org/0000-0001-6744-929X>

References

- [1] Y. Liu, J. Jia, T. Gao, X. Wang, J. Yu, D. Wu and F. Li, *J. Chem. Eng. Data* **65**, 3998 (2020). doi:10.1021/acs.jced.0c00318.
- [2] A.A. Bhatti, M. Oguz and M. Yilmaz, *J. Chem. Eng. Data* **62**, 2819 (2017). doi:10.1021/acs.jced.7b00128.
- [3] S. Memon, A.A. Bhatti, A.A. Bhatti and I.B. Solangi, *Desalin. Water Treat.* **57**, 1844 (2016). doi:10.1080/19443994.2014.993723.
- [4] H. Mahmoodian, O. Moradi, B. Shariatzadeha, T.A. Salehf, I. Tyagi, A. Maity, M. Asif and V. K. Gupta, *J. Mol. Liq.* **202**, 189 (2015). doi:10.1016/j.molliq.2014.10.040.
- [5] D. Robati, B. Mirza, M. Rajabi, O. Moradi, I. Tyagi, S. Agarwal and V. Gupta, *Chem. Eng. J.* **284**, 687 (2016). doi:10.1016/j.cej.2015.08.131.
- [6] T. Shahzadi, S. Rehman, T. Riaz and M. Zaib, *Int. J. Environ. Anal. Chem.* **2020**, 1. doi: 10.1080/03067319.2020.1789610.
- [7] M. Ghaedi, M. reza Rahimi, A. Ghaedi, I. Tyagi, S. Agarwal and V.K. Gupta, *J. Colloid Interface Sci.* **461**, 425 (2016). doi:10.1016/j.jcis.2015.09.024.
- [8] M. Ghaedi, M. Roosta, A. Ghaedi, A. Ostovan, I. Tyagi, S. Agarwal and V.K. Gupta, *Res. Chem. Intermed.* **44**, 2929 (2018). doi:10.1007/s11164-015-2285-x.
- [9] S. Agarwal, H. Sadegh, M. Monajjemi, A.S. Hamdy, G.A. Ali, A.O. Memar, R. Shahryarighoshekandi, I. Tyagi and V.K. Gupta, *J. Mol. Liq.* **218**, 191 (2016). doi:10.1016/j.molliq.2016.02.060.
- [10] S. Agarwal, I. Tyagi, V.K. Gupta, N. Ghasemi, M. Shahivand and M. Ghasemi, *J. Mol. Liq.* **218**, 208 (2016). doi:10.1016/j.molliq.2016.02.073.
- [11] D. Robati, B. Mirza, R. Ghazisaeidi, M. Rajabi, O. Moradi, I. Tyagi, S. Agarwal and V.K. Gupta, *J. Mol. Liq.* **216**, 830 (2016). doi:10.1016/j.molliq.2016.02.004.
- [12] A.M. Starvin, Doctoral dissertation, Cochin Univ. Sci.Technol. **2005**.
- [13] A. Katz, P. Da Costa, A.C.P. Lam and J.M. Notestein, *Chem. Mater.* **14**, 3364 (2002). doi:10.1021/cm020082l.
- [14] R. Junejo, N.S. Jalbani, S. Memon, S. Kaya, S. Erkan, G.L. Serdaroglu and I.M. Palabiyik, *J. Chem. Eng.* **66**, 379-388. *Data* **2020**.
- [15] R. Junejo, S. Memon, F. Durmaz, A.A. Ahmed, F.N. Memon, N.S. Jalbani, S.S. Memon and A. A. Bhatti, *Adv. J. Chem.-Sect. A* **3**, 680 (2020).
- [16] R. Junejo, S. Memon and I.M. Palabiyik, *Eurasian Chem. Commun.* **2**, 785 (2020). doi:10.33945/SAMI/ECC.2020.7.6.
- [17] C.D. Gutsche, *Calixarenes: An Introduction* (Royal Society of Chemistry, Cambridge, 2008).

- [18] M.-Z. Asfari, V. Böhmer, J. Harrowfield and J. Vicens, *Calixarenes 2001* (Kluwer Academic Publishers, New York, 2007).
- [19] N.S. Jalbani, A.R. Solangi, S. Memon, R. Junejo, A.A. Bhatti, M.L. Yola, M. Tawalbeh and H. Karimi-Maleh, *J. Mol. Liq.* **2021**, 116741. doi:10.1016/j.molliq.2021.116741
- [20] M.A. Kamboh, I.B. Solangi, S. Sherazi and S. Memon, *Desalination* **268**, 83 (2011). doi:10.1016/j.desal.2010.10.001.
- [21] M.A. Kamboh, I.B. Solangi, S. Sherazi and S. Memon, *J. Hazard. Mater.* **186**, 651 (2011). doi:10.1016/j.jhazmat.2010.11.058.
- [22] S. Memon, A.A. Bhatti and A.A. Bhatti, *Polycycl. Aromat. Compd.* **39**, 238 (2019). doi:10.1080/10406638.2017.1306571.
- [23] N.Z. Rosly, A.H. Abdullah, M. Ahmad Kamarudin, S.E. Ashari and S.A. Alang Ahmad, *Int. J. Environ. Res. Public Health* **18**, 397 (2021). doi:10.3390/ijerph18020397.
- [24] H. Li, H. Huang, X. Yan, C. Liu and L. Li, *Mater. Chem. Phys.* **263**, 124295 (2021). doi:10.1016/j.matchemphys.2021.124295.
- [25] R. Junejo, S. Memon, F.N. Memon, A.A. Memon, F. Durmaz, A.A. Bhatti and A.A. Bhatti, *J. Chem. Eng. Data* **64**, 3407 (2019). doi:10.1021/acs.jced.9b00223.
- [26] R. Junejo, S. Memon and S. Kaya, *J. Chem. Eng. Data* **65**, 4805 (2020). doi:10.1021/acs.jced.0c00292.
- [27] R. Junejo, N. Shams Jalbani, S. Kaya, G. Serdaroglu, S. Şimşek and S. Memon, *Sep Sci Technol* **2021**, 1. doi:10.1080/01496395.2021.1900252
- [28] C.D. Gutsche, M. Iqbal and D. Stewart, *J. Org. Chem.* **51**, 742 (1986). doi:10.1021/jo00355a033.
- [29] C.D. Gutsche and L.-G. Lin, *Tetrahedron* **42**, 1633 (1986). doi:10.1016/S0040-4020(01)87580-3.
- [30] J.S. Al-Otaibi, Y.S. Mary, Y.S. Mary, S. Kaya and S. Erkan, *J. Mol. Liq.* **317**, 113924 (2020). doi:10.1016/j.molliq.2020.113924.
- [31] S. Erkan and D. Karakaş, *J. Mol. Struct.* **1199**, 127054 (2020). doi:10.1016/j.molstruc.2019.127054.
- [32] R.G. Parr, L.V. Szentpály and S. Liu, *J. Am. Chem. Soc.* **121**, 1922 (1999). doi:10.1021/ja983494x.
- [33] J.L. Gazquez, A. Cedillo and A. Vela, *J. Phys. Chem. A* **111**, 1966 (2007). doi:10.1021/jp065459f.
- [34] M. Kamboh, I. Solangi, S. Sherazi and S. Memon, *J. Iran. Chem. Soc.* **8**, 272 (2011). doi:10.1007/BF03246224.
- [35] M.A. Kamboh, W.A. Wan Ibrahim, H. Rashidi Nodeh, L.A. Zardari, S.T.H. Sherazi and M. M. Sanagi, *Sep Sci Technol* **54**, 2240 (2019). doi:10.1080/01496395.2018.1543322.
- [36] E. Akceylan, M. Bahadir and M. Yılmaz, *J. Hazard. Mater.* **162**, 960 (2009). doi:10.1016/j.jhazmat.2008.05.127.
- [37] S. Rattanaphani, M. Chairat, J.B. Bremner and V. Rattanaphani, *Dyes Pigm.* **72**, 88 (2007). doi:10.1016/j.dyepig.2005.08.002.
- [38] S. Kaya and C. Kaya, *Comput. Theor. Chem.* **1060**, 66 (2015). doi:10.1016/j.comptc.2015.03.004.
- [39] S. Kaya, C. Kaya and N. Islam, *Physica B Condens. Matter* **485**, 60 (2016). doi:10.1016/j.physb.2016.01.010.
- [40] A. Singh, K. Ansari, M. Quraishi, S. Kaya and S. Erkan, *Int. J. Hydrogen Energy* **46**, 9452 (2021). doi:10.1016/j.ijhydene.2020.12.103.
- [41] Y. Yang, J. Yang, Y. Du, C. Li, K. Wei, J. Lu, W. Chen and L. Yang, *ACS Omega* **4**, 17741 (2019). doi:10.1021/acsomega.9b02180.
- [42] S. Shahabuddin, N.M. Sarih, M. Afzal Kamboh, H. Rashidi Nodeh and S. Mohamad, *Polymers* **8**, 305 (2016). doi:10.3390/polym8090305.
- [43] H. Chen, J. Zhao, J. Wu and G. Dai, *J. Hazard. Mater.* **192** (1), 246 (2011).